

NASA/CR—2005-213965



# Intelligent Engine Systems

## Work Element 1.3: Sub System Health Management

Malcolm Ashby, Jeffrey Simpson, Anant Singh, and Emily Ferguson  
General Electric Aircraft Engines, Cincinnati, Ohio

Mark Frontera  
General Electric Global Research Center, Niskayuna, New York

## The NASA STI Program Office . . . in Profile

Since its founding, NASA has been dedicated to the advancement of aeronautics and space science. The NASA Scientific and Technical Information (STI) Program Office plays a key part in helping NASA maintain this important role.

The NASA STI Program Office is operated by Langley Research Center, the Lead Center for NASA's scientific and technical information. The NASA STI Program Office provides access to the NASA STI Database, the largest collection of aeronautical and space science STI in the world. The Program Office is also NASA's institutional mechanism for disseminating the results of its research and development activities. These results are published by NASA in the NASA STI Report Series, which includes the following report types:

- **TECHNICAL PUBLICATION.** Reports of completed research or a major significant phase of research that present the results of NASA programs and include extensive data or theoretical analysis. Includes compilations of significant scientific and technical data and information deemed to be of continuing reference value. NASA's counterpart of peer-reviewed formal professional papers but has less stringent limitations on manuscript length and extent of graphic presentations.
- **TECHNICAL MEMORANDUM.** Scientific and technical findings that are preliminary or of specialized interest, e.g., quick release reports, working papers, and bibliographies that contain minimal annotation. Does not contain extensive analysis.
- **CONTRACTOR REPORT.** Scientific and technical findings by NASA-sponsored contractors and grantees.

- **CONFERENCE PUBLICATION.** Collected papers from scientific and technical conferences, symposia, seminars, or other meetings sponsored or cosponsored by NASA.
- **SPECIAL PUBLICATION.** Scientific, technical, or historical information from NASA programs, projects, and missions, often concerned with subjects having substantial public interest.
- **TECHNICAL TRANSLATION.** English-language translations of foreign scientific and technical material pertinent to NASA's mission.

Specialized services that complement the STI Program Office's diverse offerings include creating custom thesauri, building customized databases, organizing and publishing research results . . . even providing videos.

For more information about the NASA STI Program Office, see the following:

- Access the NASA STI Program Home Page at <http://www.sti.nasa.gov>
- E-mail your question via the Internet to [help@sti.nasa.gov](mailto:help@sti.nasa.gov)
- Fax your question to the NASA Access Help Desk at 301-621-0134
- Telephone the NASA Access Help Desk at 301-621-0390
- Write to:  
NASA Access Help Desk  
NASA Center for AeroSpace Information  
7121 Standard Drive  
Hanover, MD 21076

NASA/CR—2005-213965



# Intelligent Engine Systems

## Work Element 1.3: Sub System Health Management

Malcolm Ashby, Jeffrey Simpson, Anant Singh, and Emily Ferguson  
General Electric Aircraft Engines, Cincinnati, Ohio

Mark Frontera  
General Electric Global Research Center, Niskayuna, New York

Prepared under Contract NAS3-01135

National Aeronautics and  
Space Administration

Glenn Research Center

---

October 2005

Available from

NASA Center for Aerospace Information  
7121 Standard Drive  
Hanover, MD 21076

National Technical Information Service  
5285 Port Royal Road  
Springfield, VA 22100

Available electronically at <http://gltrs.grc.nasa.gov>

# Contents

1. Introduction .....	1
1.1. Objectives .....	1
1.2. Report Outline .....	1
1.3. Report Summaries .....	1
1.3.1. Start sub-system health management .....	1
1.3.2. Oil sub-system health management .....	1
1.3.3. Bearings sub-system health management .....	1
1.3.4. Fuel sub-system health management .....	2
2. Subtask: Starting System .....	2
2.1. Background .....	2
2.2. Approach .....	2
2.3. Characterization of Major Faults of Jet Engine Starter and Ignition Systems.....	2
2.4. Develop Physics-Based Fault-Detection Model Requirements.....	3
2.4.1. Baseline model modifications.....	3
2.4.2. Model operating requirements .....	3
2.5. Start Process .....	4
2.6. Model Inputs.....	5
2.6.1. Starter pressure and temperature.....	5
2.6.2. Random ambient conditions .....	5
2.6.3. Random engine to engine degradation.....	5
2.6.4. Random subsystem variation .....	5
2.7. Fault Simulations.....	5
2.7.1. Starter faults .....	5
2.7.2. Hydro-mechanical unit fault .....	6
2.7.3. Igniter/exciter fault.....	6
2.8. Sensor Monitoring and Sampling .....	6
2.9. Monte Carlo Run Setup and Execution .....	6
2.10. Fault Detection .....	6
2.10.1. Statistical basics .....	6
2.10.2. Fault library.....	7
2.11. Fault Isolation.....	8
2.11.1. Generation of confusion matrix .....	8
2.12. Performance Summary .....	8
2.12.1. Definition of performance metrics:.....	8
2.13. Recommended Next Steps – Phase II.....	9
2.13.1. Tracking filter .....	9
2.13.2. Validate with real start data .....	9
2.13.3. A priori probability .....	9
3. Subtask: Oil System .....	9
3.1. Background .....	9
3.2. Approach .....	9
3.3. Characterize Major Faults of Jet Engine Oil Systems.....	10
3.4. Develop Physics-Based Fault-Detection Model Requirements.....	11
3.4.1. Model selection.....	11
3.4.2. Lube system general description.....	11
3.4.3. Baseline model modifications.....	12
3.4.4. Model operating requirements .....	12
3.5. Baseline Models .....	12

3.5.1. Lubrication oil supply model .....	13
3.5.1.1. Assumptions .....	14
3.5.1.1.1. Failed O-ring assumptions .....	14
3.5.1.2. Results .....	14
3.5.1.3. Conclusions .....	14
3.5.1.4. Rig model results .....	14
3.5.1.5. Rig model conclusions .....	14
3.5.1.6. Failed O-ring model .....	14
3.5.1.7. Failed O-ring results .....	14
3.5.2. Scavenge model .....	15
3.5.2.1. Assumptions .....	15
3.5.2.1.1. Broken Scavenge Tube Assumptions .....	15
3.5.2.1.2. Failed Carbon Seal Assumptions .....	16
3.5.2.1.3. Component Failure Assumptions.....	16
3.5.2.2. Master engine scavenge model results .....	16
3.5.2.3. Master engine scavenge model conclusions .....	16
3.5.2.4. Lube test vehicle scavenge model results.....	16
3.5.2.5. Lube test vehicle model conclusions .....	16
3.5.2.6. Increased airflow failure vented sump model results .....	16
3.5.2.7. Increased airflow failure model conclusions .....	17
3.6. Conclusion : Oil Systems .....	17
4. Subtask: Bearing System .....	17
4.1. Background .....	17
4.2. Approach .....	18
4.3. Define Sensing Requirements .....	18
4.4. Identify Available Sensor Technologies.....	19
4.5. Develop State-Awareness Sensors .....	19
4.5.1. Bearing outer race sensors .....	19
4.5.2. Instrumentation system .....	20
4.5.3. Test rig configuration.....	20
4.6. Demonstrate Sensing Concept in Laboratory Environment .....	20
4.6.1. Test plan.....	20
4.6.2. Test results and discussion.....	20
5. Subtask: Fuel System .....	23
5.1. Background .....	23
5.2. Approach .....	23
5.3. Characterization of Major Faults of Jet Engine Starter and Ignition Systems.....	23
5.4. Develop Physics-Based Fault-Detection Model Requirements.....	23
5.4.1. Model selection .....	23
5.4.2. General requirements .....	24
5.4.3. Model operating requirements .....	24
5.5. Modeling of The Fuel System For Real-Time Detection of Selected Faults .....	25
5.5.1. Argo-tech models.....	25
5.5.2. GEAE models .....	28
5.5.3. Fault injection capability.....	28

## Figures

Figure 2.5-1 Ground start unbalance torque diagram .....	4
Figure 2.10.1-1 Definition of statistical significance.....	7
Figure 2.10.1-2 Sample histogram of Monte Carlo simulation .....	7
Figure 2.12.1-1 Predicted model performance.....	9
Figure 3.3-1 Process used to identify candidate lube problems for modeling .....	10
Figure 3.4.2-1 Lubrication system schematic .....	11
Figure 3.4.3-1 Sump modeling approach.....	13
Figure 4.5.2-1 Sensor interconnection and data processing.....	21
Figure 4.5.3-1 Test rig arbor and slip ring bearing sub-assembly .....	21
Figure 4.5.3-2 Assembled bearing test rig .....	22
Figure 4.6.2-1 Measured versus calculated RPFO (Undamaged Brg – constant speed).....	22
Figure 5.4.1-1 Fuel system schematic.....	24
Figure 5.5.1-1 Generic actuator top-level model representation.....	26
Figure 5.5.1-2 Heat exchanger test circuit .....	26
Figure 5.5.1-3 Example heat exchanger effectiveness versus fuel flow .....	27
Figure 5.5.1-4 Example heat exchanger pressure drop characteristic.....	27
Figure 5.5.1-5 Example heat exchanger top-level model representation.....	28
Figure 5.5.2-1 Fuel flowmeter pressure drop characteristics.....	29
Figure 5.5.2-2 Manifold pressure characteristic comparison.....	29

## Tables

Table 2.11.1-1 General form of confusion matrix .....	8
Table 3.5.1.7-1 Failed O-ring results summary .....	15
Table 5.5-1 Fuel system modeling tasks.....	25



# Intelligent Engine Systems

## Work Element 1.3: Sub System Health Management

### 1. Introduction

#### 1.1. Objectives

The objectives of this program were to develop health monitoring systems and physics-based fault detection models for engine sub-systems including the start, lubrication, and fuel. These models will ultimately be used to provide more effective sub-system fault identification and isolation to reduce engine maintenance costs and engine down-time.

Additionally, the bearing sub-system health is addressed in this program through identification of sensing requirements, a review of available technologies and a demonstration of a conceptual monitoring system for a differential roller bearing.

#### 1.2. Report Outline

This report is divided into 4 sections; one for each of the subtasks. The start system subtask is documented in section 2.0, the oil system is covered in section 3.0, the bearings in section 4.0 and finally the fuel system is presented in section 5.0.

#### 1.3. Report Summaries

The work elements for each of the four tasks that comprised Work Element 1.3 are summarized in the following paragraphs.

##### 1.3.1. Start sub-system health management

The primary work elements for this task were as follows:

- A. Characterization of the major faults of jet engine starter/ignition systems.
- B. Development of physics-based fault-detection model requirements.
- C. Provision of a Base Engine Model.
- D. Modeling of the starter system for real-time detection of selected faults.

##### 1.3.2. Oil sub-system health management

The primary work elements for this task were as follows:

- A. Characterization of the major faults of jet engine oil systems.
- B. Development of physics-based fault-detection model requirements.
- C. Modeling of the oil system for real-time detection of selected faults.
- D. Support Rig Planning for potential phase 2 verification efforts.

##### 1.3.3. Bearings sub-system health management

The primary work elements for this task were as follows:

- A. Define sensing requirements.
- B. Identify available sensing technologies.
- C. Develop state-awareness sensors.
- D. Demonstrate sensing concept in a laboratory environment.

### **1.3.4. Fuel sub-system health management**

The primary work elements for this task were as follows:

- A. Characterization of the major faults of large turbofan fuel systems.
- B. Development of physics-based fault-detection model requirements.
- C. Modeling of the fuel system for real-time detection of selected faults.

## **2. Subtask: Starting System**

### **2.1. Background**

Aircraft engine start system failures and subsequent troubleshooting because a significant portion of propulsion related airline delays and cancellations. The objective of this task was to develop a physics-based model of the start system to determine fault detection and isolation performance. The eventual goal is to reduce the maintenance and delays and cancellation.

### **2.2. Approach**

Key start system faults were identified via historical fault databases and Failure Modes and Effects Analyses (FMEA). These faults were reviewed for modeling suitability and a short list generated. A successful start is dependent on the health of the entire engine system, including the turbo-machinery, start subsystem, ignition subsystem, and fuel subsystem. Thus, a pre-existing model was chosen as the baseline for a physics-based model for starting fault detection. Numerous improvements were made to this baseline model and the faults previously down-selected were modeled. Since a baseline model was already available for this task, efforts were re-directed at evaluating the performance of fault detection and isolation techniques.

### **2.3. Characterization of Major Faults of Jet Engine Starter and Ignition Systems**

Utilizing a database of documented commercial engine starting system repairs and maintenance, valuable information about engine performance and fault occurrences were analyzed and fault-prone parts were identified.

For the starter system related faults the Starter Air Valve was the source of the most frequently occurring fault. Also, it is highly probable and practical that detection methods could be developed to detect malfunctions in the Start Valve. The Starter was also included in this list, because a significant number of malfunctions were detected. Many times, the reason for replacement of the Starter is documented as “TBD,” suggesting that diagnosis of the Starter may be more difficult.

For the ignition system related faults, the Igniter dominated as the most often replaced part. In all cases, the Igniter showed signs of misdiagnosis or inadequate diagnosis with a high occurrence of “Multiple LRU Replaced,” which provides a strong case for improving isolation methods for this part.

With regards to the fuel system, the Hydromechanical Unit (HMU) was replaced most often. Here also a relatively high occurrence of “Multiple LRU Replaced” was noted, indicating inadequate diagnosis.

FMEA’s were then consulted to identify the primary fault-prone parts and used to help understand the context behind how these parts often fail.

Based on the above findings, the list was narrowed down to a only a handful of engine parts that consistently cause major problems, but at the same time may be monitored effectively. The following is the list, ranked in order of most prevalent.

- Starter Air Valve
- HMU
- Igniter
- Starter

## **2.4. Develop Physics-Based Fault-Detection Model Requirements**

The original program assumption was that a start model would need to be developed from scratch. However in the early portion of the effort we became aware of an existing physics based engine cycle model that had some start capability and this was leveraged for this program.

### **2.4.1. Baseline model modifications**

Some modifications to the baseline model and input files were required before it could be used for fault detection. In order to represent the large variation in operating environment and engine-to-engine variation, the following was added to the model:

- Engine thermal state impact (hot starts versus cold starts)
- Correlation between Starter inlet pressure/temperature and ambient conditions
- Engine deterioration factors

The model was also modified to implement the following faults:

- SAV failed to close or partially open.
- Starter low torque due to blade or clutch damage.
- Rich or lean fuel flow due to HMU or FADEC fault.
- Delays in engine light off—simulating poor igniter performance.

Originally, the decision was made not to model any ignition faults since most ignition faults result in no light off. This would have been a trivial effect to include in this model. The impacts due to delayed light off affects the overall start process, so this capability was subsequently incorporated.

A fault isolation tree was used to determine the minimum number of sensors or metrics required to isolate the fault to a component. The model outputs were updated to output the following sensor outputs/metrics:

- Motoring time
- SAV sensor output
- Compressor Core speed and Acceleration
- Fuel flow signal
- Exhaust gas temperature
- Overall start time

### **2.4.2. Model operating requirements**

This study was focused primarily on ground starts, as this is the overwhelming majority of all starts. Therefore, the model was utilized in the following ground starting envelope:

- Altitude: -2000 to 7000 ft
- Ambient temperature: -40 to 120 °F
- Oil Temperature: Ambient temperature (for cold starts) to 200 °F (for hot starts)
- Thermal state of the engine.

Actual starting envelope requirements for component design purposes are more extreme; however, this range covers greater than 95 percent of ground starts.

## 2.5. Start Process

Before discussing the fault detection and isolation approaches studied in this program, it is necessary to understand the engine start process. Figure 2.5–1 highlights a basic aircraft engine start procedure.

Referring to figure 2.5–1:

1. Air turbine starter is powered up, and begins turning the engine. The torque required to accelerate the engine increases with rotor speed as an effect of the increase in airflow (drag forces, pumping forces, etc.).
2. Before reaching the maximum motoring point, fuel is added and the igniter begins to spark. This point is determined by a low-threshold rotor speed. (Maximum motoring point: the stage of starter output torque equal to the engine unfired torque)
3. Once light off occurs and a flame is sustained, the engine begins to accelerate the system. (High-Pressure Turbine (HPT) is now doing work).
4. At the self-sustaining point, the torque is balanced (in theory). At any point prior to the self-sustaining point, disengaging the starter would not allow the engine to achieve idle engine speed. The HPT is now extracting enough work to keep the compressor at a constant speed without the help of the starter. The starter does not cutout at this point.
5. More fuel is added, accelerating the engine to idle speed. The starter assists through a portion of this acceleration to reduce the time to idle. At a high threshold rotor speed the starter disengages, and the HPT powers the engine speed to idle.

### System Faults

As illustrated on figure 2.5–1, 3 key fault types are detectable at different points in the start procedure.

**Starter Fault.**—This fault type is detectable from the onset of the start cycle. Any failure in the starter system will impact output starter torque and engine core speed from the first stage of the start process.

**Fuel System Fault.**—This fault type is detectable at the onset of fuel flow, just prior to ignition. A failure in this system may impact time of ignition, engine core speed, or exhaust gas temperature.

**Ignition System Fault.**—This fault type is detectable at engine light off. It is detectable through transient delays in the start light-off procedure.

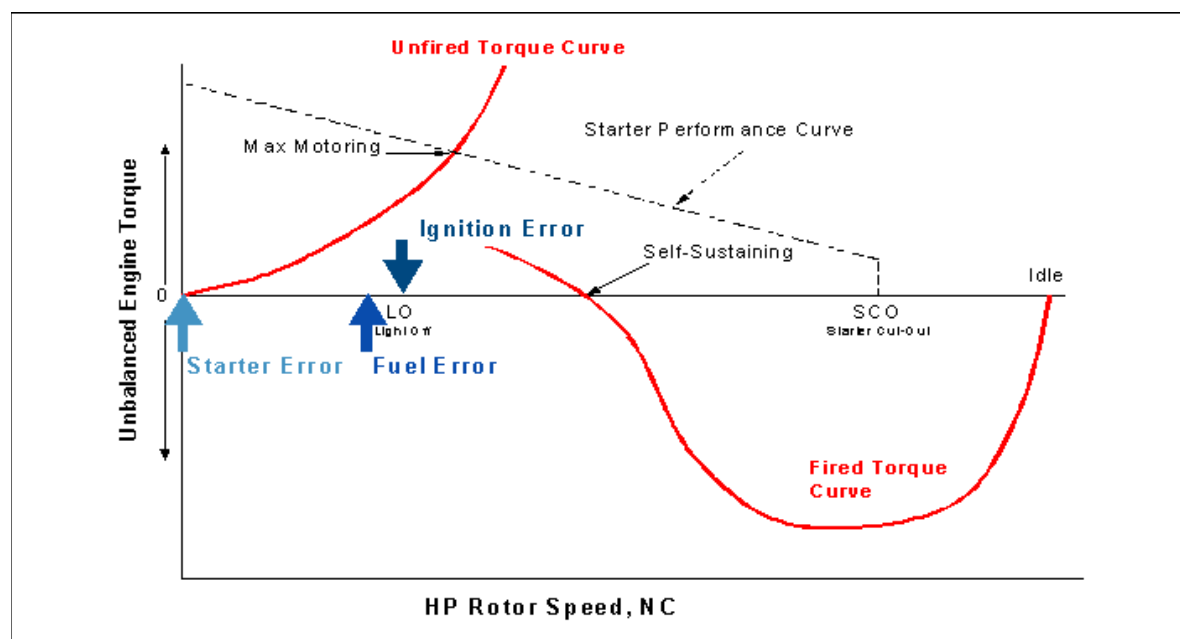


Figure 2.5–1.—Ground start unbalance torque diagram.

## 2.6. Model Inputs

The following model input capabilities were provided.

### 2.6.1. Starter pressure and temperature

Model inputs for Starter Pressure and Temperature from the APU are predicted by a transfer function generated from starter inlet data.

### 2.6.2. Random ambient conditions

Both simulation and validation procedures use randomized ambient temperature and altitude for each Monte Carlo simulation point. Randomization was generated using Matlab's random number generator across the environmental ranges presented above. For each random case, a hot start and cold start was run.

### 2.6.3. Random engine to engine degradation

Each engine produced varies slightly from other engines of the same series, and will degrade over many flight cycles. Random engine variation and degradation modeling was induced using Matlab's random number generator.

### 2.6.4. Random subsystem variation

Three subsystems critical to the start process were modeled with random component variation as follows:

- Fuel System
- Starter Degradation
- Ignition Delay

The variation was included in the Monte Carlo Simulation and the 'Real Engine' Model of the validation.

## 2.7. Fault Simulations

### 2.7.1. Starter faults

Variation of starter torque was simulated by three start system faults: Starter Torque Mechanical degradation, Starter Air Valve, and Air Passage Blockage faults. This fault type impacts the output torque of air turbine starter. This fault impacts the entire start process.

1. Starter Mechanical Degradation
  - Starter torque is a function of pressure, temperature and shaft speed. A fault caused by the mechanical fault (deterioration) in the starter turbine is simulated by a direct scaling factor on torque.
2. Starter Air Valve Failure and Blockage Fault
  - Output starter torque may also be influenced by restriction of airflow from the Auxiliary Power Unit to the Starter Air Turbine. Two potential causes of this knockdown were modeled; simulating an incomplete opening of the starter air valve and simulation of an obstruction in the air passage.
  - The partially opened Starter Air Valve (SAV) was simulated through a pressure drop across the SAV. The pressure variation was a function of change in effective area caused by the partially opened valve.
  - An obstruction in the air passage was modeled using a direct percent scalar on the effective area. This also caused a change in the pressure drop across the Starter Air Valve.

### 2.7.2. Hydro-mechanical unit fault

Malfunctions in the Hydro-Mechanical Unit (HMU) can lead to an off-schedule fuel flow being applied to the engine. A direct scalar on engine fuel flow simulates degradation or enhancement of fuel flow.

### 2.7.3. Igniter/exciter fault

A failure in the Igniter/Exciter Fault is simulated through combustion ignition delay. The fault routine delays ignition for a user defined input time (seconds).

## 2.8. Sensor Monitoring and Sampling

The following sensors were identified as critical to monitor during the start window.

- Fuel Flow
- Exhaust Gas Temperature
- Engine Core Speed
- Engine Core Acceleration
- Starter Cutoff Time
- Starter Pressure
- Starter Torque: model dependent, not Real Engine Sensor

These sensors were used for Fault Isolation Logic and were chosen based on the impact of capturing starter system fault types.

## 2.9. Monte Carlo Run Setup and Execution

Environmental, engine degradation, component variation, and fault types were randomized for the Monte Carlo simulation using a file input/output structure in Matlab.

Following the execution of the Monte Carlo Simulation, the data was fed into Matlab using an automated routine. Once input into Matlab, differences are taken between the engine test data and nominal data for each environmental condition. These differences are the inputs for fault signature analysis and storage.

## 2.10. Fault Detection

### 2.10.1. Statistical basics

Statistical significance is a measure of confidence quantifying the probability of an incorrect declaration. A common metric used for statistical significance between two data sets is the Z-score.

Figure 2.10.1-1 illustrates two Gaussian distributions with a small overlap area. The red distribution contains data produced by a faulted model, whereas the green distribution represents data produced a no-fault model. A data point falling to the left of the Gaussian intersection is classified as a fault, while a point falling to the right of the curve intersection is classified as a good start.

Z is defined as:

$$Z = (x - \mu) / \sigma$$

Where: x is distance from the mean,  $\mu$ .  
 $\sigma$  is standard deviation

The threshold, x was chosen to balance Type I and Type II errors.

- A Type I error is a False Alarm, the probability of claiming a fault occurred when the start process was a good start.
- A Type II error is a Missed Fault, the probability of claiming a good start, when a fault occurred.

Z-score increases as the separation between the two data sets increases or as the standard deviation of each set decreased. A high Z-score allows a claim of fault or no fault to be made with significant confidence.

Figure 2.10.1–2 represents the overlap of three Gaussian distributions occurring in the engine model. The red and blue data distributions are a snapshot of Monte Carlo run data at a single time point. In comparison, the green data set represents a good start at the same time step. From this illustration, fault 2 (red) has a larger separation and smaller standard deviation than fault 1 (blue) when compared to the good start (green). This states that fault 2 is more statistically detectable from a good start, when compared to fault 1.

### 2.10.2. Fault library

For each fault case (type and magnitude) the average sensor readings, Z Score, Threshold, and Covariance Matrix, are stored into a Fault Storage Library.

Currently, the listed fault types and magnitudes are stored in individual data files and read into Matlab into a fault library matrix. Additional faults or multiple fault cases may be run as new Monte Carlo simulations and added to the Fault Library.

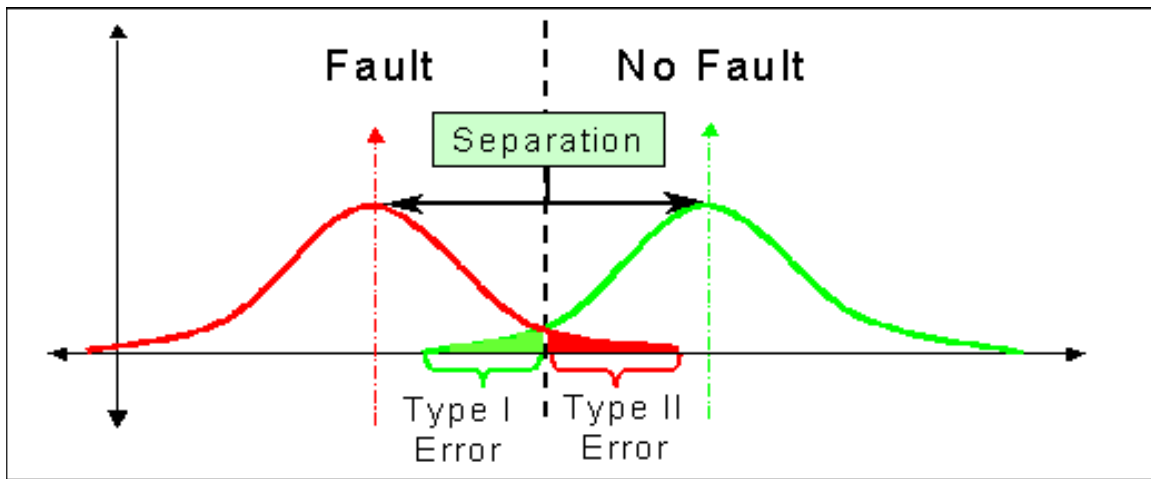


Figure 2.10.1–1.—Definition of statistical significance.

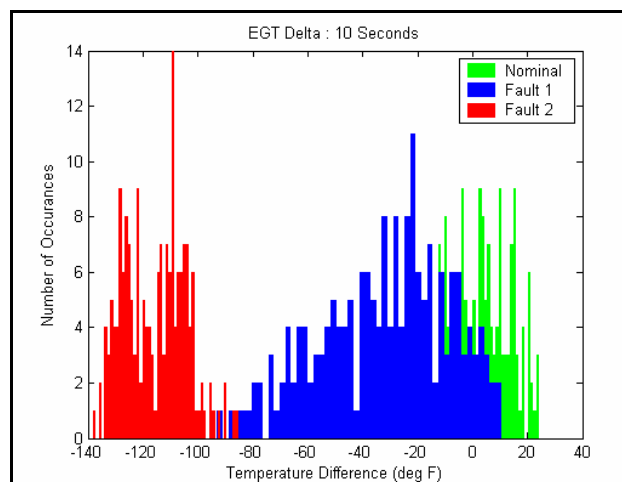


Figure 2.10.1–2.—Sample histogram of Monte Carlo simulation.

## 2.11. Fault Isolation

Confidence of the decision must be defined taking other possible fault signatures into consideration. The probability of being any other identifiable fault is now introduced as another error type; missed diagnosis.

### 2.11.1. Generation of confusion matrix

A Landscaping Analysis performed on Mechanical Starter Faults and Fuel System Faults dictated the need to quantify the isolation between faults; the development of a confusion matrix. A confusion matrix compares the probability of selecting a fault to the actual fault/no fault occurrence.

TABLE 2.11.1-1.—GENERAL FORM OF CONFUSION MATRIX

Actual	Predicted		
	0	1	2
0	P(0 0)	P(1 0)	P(2 0)
1	P(0 1)	P(1 1)	P(2 1)
2	P(0 2)	P(1 2)	P(2 2)

Many decisions may be inferred using the Confusion Matrix presented in table 2.11.1-1.

Example of decisions inferred from Confusion Matrix:

- False Alarm Rate =  $P(0|0) = 1 - (P(1|0) + P(2|0))$
- Missed Fault Rate =  $P(0|1) + P(0|2)$

Overall the confusion table generated for this program highlighted the need for a reduction in variance in order to improve the detection rate of smaller order of magnitude faults, and/or to reduce the magnitude of the smallest detectable fault.

The generation of the confusion matrix is a function of a priori information, and is calculated prior to the real-time application. The confusion matrix must be recalculated with any additions to the fault library.

## 2.12. Performance Summary

The performance of the fault detection procedure may be quantified leveraging the confusion matrix generated above. These metrics represent the upper bound performance of using these statistical methods.

### 2.12.1. Definition of performance metrics:

- Detection Rate—Probability of Declaring any Fault, when any Fault has occurred
- False Alarm Rate—Probability of Declaring a Fault, when no Fault has occurred
- Classification Rate—Probability a Fault is Correctly Identified for Fault Type and Magnitude
- Classification Rate with out Magnitude—Probability a Fault is Correctly Identified for Fault Type
- Isolation of Starter Fault—Probability of Correctly identifying any Starter Failure when any Starter Failure Occurred

Figure 2.12.1-1 presents results for the five key parameters used to quantify the system performance.

These probabilities may be enhanced with a reduction in system variation. As additional faults are added to the library, additional sensors may be required to increase the accuracy of the prediction.

**Predicted Performance:**  
**Detection Rate : 97.73%**  
**False Alarm Rate : 10.61%**  
**Classification Rate: 70.98%**  
**Classification Rate w/o Magnitude : 88.26%**  
**Isolation of Starter Fault : 95.02%**

Figure 2.12.1-1.—Predicted model performance.

### **2.13. Recommended Next Steps—Phase II**

The following recommendations are presented for future work in this area.

#### **2.13.1. Tracking filter**

The performance indicated in figure 2.12.1–1 show that a lower false alarm rate and increase in classification rate would be beneficial for application to a production fault isolation procedure. Additionally, the confusion matrix illustrated the need to improve low-magnitude fault isolation.

With perfect tracking, engine and component degradation would be removed from the simulation of the real engine in the a priori fault library generation.

#### **2.13.2. Validate with real start data**

This analysis substituted a simulation for real engine data. To ensure the predicted process performance, validation to real engine start data is required. Starter mechanical, fuel system, and ignition delay faults would be validated using transient start data.

#### **2.13.3. A priori probability**

A priori probability would enable previous knowledge of the health of engine components to be weighted into fault isolation decisions. If a specific starter has a high probability of starter fault, in comparison to fuel fault, this knowledge may be added to the decision making process. The introduction of Reasoners to this process may enhance the predictive performance.

## **3. Subtask: Oil System**

### **3.1. Background**

Analysis reveals that approximately 8 to 9 percent of propulsion related commercial airline delays and cancellations are due to oil system problems. The objective of this task was to develop a physics-based model of the oil system for the purpose of fault detection and isolation.

### **3.2. Approach**

Key oil system faults were identified via historical fault databases and Failure Modes and Effects Analyses (FMEA). These faults were reviewed for modeling suitability and generic applicability and a summary list down-selected. A military engine oil system was selected as the candidate system for the modeling effort. This decision was made primarily because GEAE has an engine-level sump simulator rig, which will be an excellent test environment for Phase 2 of the program. The modeling included both pressure and scavenge sides of the oil system.

### 3.3. Characterize Major Faults of Jet Engine Oil Systems

A review of historical information using data from 1988–2003 from commercial engines database and 1994–2003 from military engine event data was completed. Key oil system component failures (issue) in the lube system were identified along with an expected fault set (flag). The lube “flags” are problems observed by the pilot or ground crew that would result in a maintenance action. Lube “issue” is the root cause for the “flag.” A total of 1160 events were reviewed to assemble the list of “issues” to model. Data comprised 777 commercial events and 383 military engine events. Component improvement programs were also reviewed.

The flow chart illustrated in figure 3.3–1 outlines the process used to determine which failures to model.

The major lube issues were evaluated to determine major flags associated with each issue and also compared against the engine type.

This process was conducted for each of 6 issues. Only 1 issue, Labyrinth Seal Failures was found to be engine specific. Labyrinth Seals are similar to carbon seals however so only carbon seal failures were modeled.

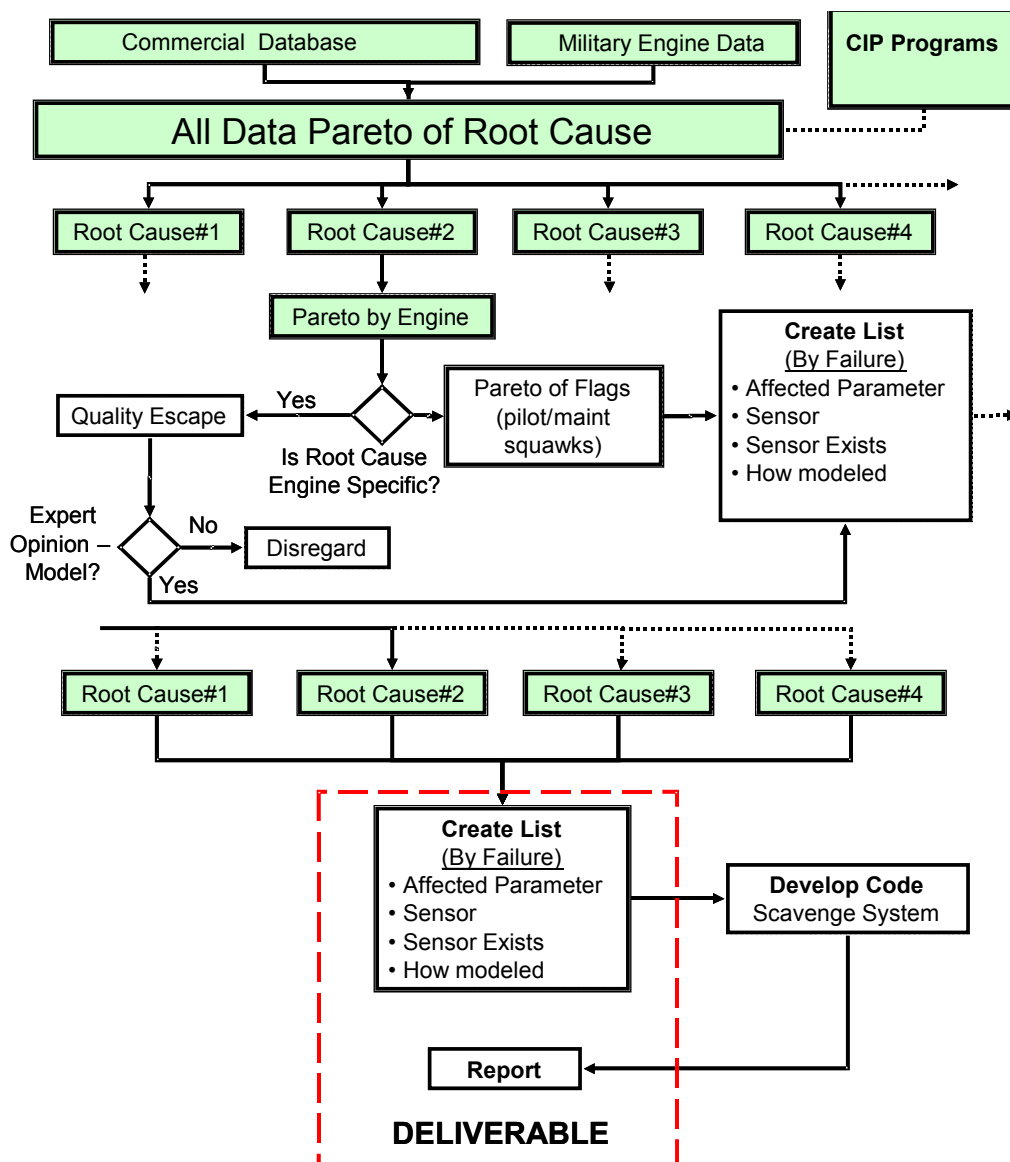


Figure 3.3.–1—Process used to identify candidate lube problems for modeling.

### 3.4. Develop Physics-Based Fault-Detection Model Requirements

#### 3.4.1. Model selection

A military engine lubrication system was chosen as the candidate system for baseline modeling. The primary reason for this is the existence of a full engine sump simulator. The overall plan is to use this simulator for validation of the model in Phase 2 of this program. The physics based model was developed in GE's FlowSim environment. The software operates on Matlab's Simulink environment and is run on a standard PC.

#### 3.4.2. Lube system general description

The engine lubrication system utilizes a pressurized, self-contained, recirculating dry sump system designed to furnish lubrication/cooling oil to the required bearings and gears during engine operation. A schematic of this system, indicating the modeling scope (supply, scavenge and shared sections of the architecture), is included as figure 3.4.2-1.

The supply line from the bottom of the oil tank is connected to the lube and scavenge pump. The oil pump is a six-element positive displacement vane pump, consisting of 1 supply element, and 5 scavenge elements. The oil is received into the pump, pressurized, filtered and exits the pump to the oil cooler.

In the oil cooler, heat is transferred from the oil to the fuel. The oil cooler is aluminum-brazed and welded oil to fuel full flow heat exchanger. The cooler contains a series of tubes containing fuel, which are immersed in oil. Heat is transferred from the hotter oil to the fuel. Fuel is ported into the cooler from the nozzle actuator fuel pump and exits to the engine fuel pump. Oil is ported through 2 exits to the A, B, and AGB sumps while the remainder of the oil flows through a different port to the C-sump.

All of the areas into which oil is delivered are scavenged by the five suction elements of the lube and scavenge pump. The combined air/oil mixture scavenged from the sump areas and gearbox is combined internally in the lube and scavenge oil pump and is ported to the top of the oil tank. In the oil tank, air is separated from the oil. Oil is ported to the bottom of the tank and air is vented through an air/oil separator in the gearbox.

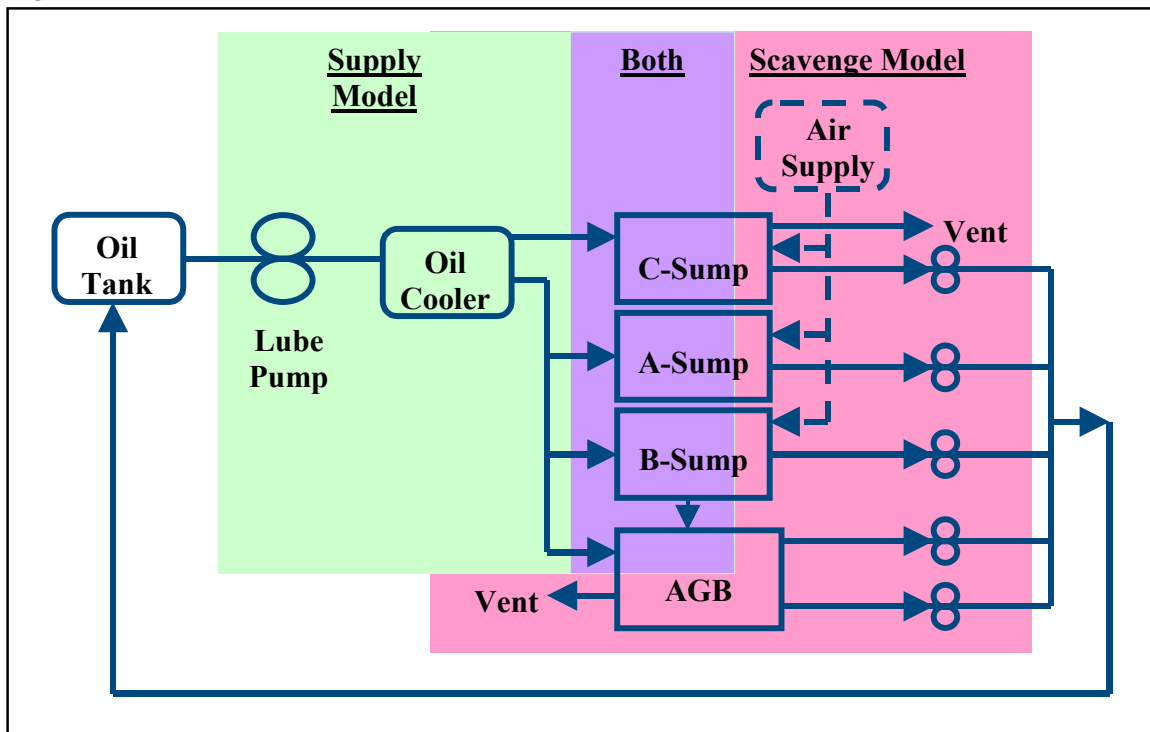


Figure 3.4.2-1.—Lubrication system schematic.

### 3.4.3. Baseline model modifications

The models operate in a steady state mode only. The models are capable of operating at most flight envelope conditions. The models are not capable of simulating attitude.

The scavenge side models have the capability to model from the sump to the scavenge pump. Downstream of the scavenge pump was not modeled, but does not affect fault detection monitoring.

The sump modeling was phased to address the complexity of two-phase flow conditions (see fig. 3.4.3–1).

Faults are incorporated into the model as follows:

- Broken tubes,
- Main shaft carbon seal failure,
- O-ring failure,
- Component failure (gearbox carbon seal).

The standard outputs from the model include: Fluid ID, Mass Flow, Temperature, and Pressure. Sensors for this model shall measure one of the above outputs.

### 3.4.4. Model operating requirements

The model operation is focused on steady state conditions, as the majority of lubrication system sensors are ignored until the lubrication system has stabilized.

Due to limitations in the test rig, all conditions must be modeled at SLS conditions with a zero (0) mach number.

<u>Condition</u>	<u>Altitude (ft)</u>	<u>Mach</u>	<u>Oil Inlet Temp (F)</u>
Flight Idle Condition	Sea Level	0	170
IRP Condition	Sea Level	0	170
MRP Condition	Sea Level	0	170

*IRP = Intermediate Rated Power*

*MRP = Maximum Rated Power*

Sump vent pressures will reference atmospheric conditions for SL, standard day. Sump seal buffer pressure inputs will be leveraged from engine test data.

## 3.5. Baseline Models

Due to the size of the model and error management requirements, the lubrication system is broken up into separate supply, vented and unvented scavenge sump models to facilitate troubleshooting and reduce run time and complexity. The lubrication system oil supply model begins from the oil pump exit and flows to each individual oil jet nozzle. All flow is incompressible, with sump pressures initially being set from engine test data and the lube schematic. The sump oil flow output of the supply model is used as input into the scavenge models. The AGB and B sumps combined all oil flows into a single oil supply entering the appropriate sump for simplification. The air entering the sump through a carbon seal uses an estimated equivalent diameter and pressure drop from engine test data to calculate flow. Oil and airflows are then mixed exiting the vent and scavenge lines appropriately. The pressures in the sump are calculated based on vent backpressure and were compared against engine test data.

The only heat addition to the lubrication oil supply model is from the mechanical efficiency losses in the lube pump and the heat rejection from the oil cooler. No other heat has been added to the oil supply model, such as heat pickup through struts or convection cooling on external supply lines. These impacts are considered negligible.

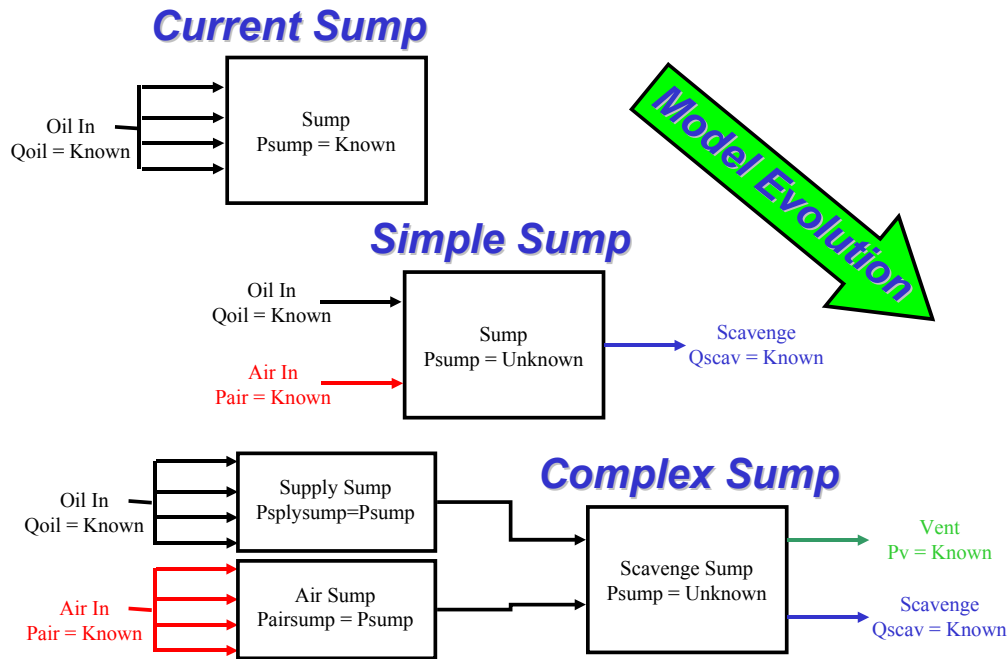


Figure 3.4.3-1.—Sump Modeling Approach.

Analysis was performed on the engine lubrication supply model input file to optimize the design. An optimized model is one, which includes significant lube supply input parameters and engine-to-engine variation. Lube and scavenge pump discharge pressure was used as the model response variable. Discharge pressure was chosen because broken tubes, carbon seal, O-ring, and scavenge pump failures will result in lube and scavenge pump discharge pressure anomalies making it ideal for measuring the ability of the model to simulate these problems.

Design trade studies were performed to develop the oil supply model input file design concept. Concepts, with and without lube supply nozzles, were compared to determine the significant lube supply parameters and if the engine oil nozzle orifice diameters could be represented by nominal values (no manufacturing variation).

Because experiments yielded similar results for concepts with and without oil nozzle orifice diameter manufacturing variation, it was determined that nozzle diameters could be set at nominal values and still get acceptable results.

### 3.5.1. Lubrication oil supply model

The supply model includes all supply components from the oil tank to the nozzle outlets into the A, B, C, and AGB sumps. The supply system oil pump flow is the oil flow entering the oil cooler. It does not include the internal lube pump lubrication since that flow is circulated back into the oil inlet side of the lube pump and never enters the scavenge system. The internals of the lube pump such as filter pressure drop and high-pressure relief valve were not modeled, but could be incorporated in the future. The engine model was validated by engine test data, drawing specifications, and air pressurization and lube schematics.

The rig engine that will be used to generate common failures in the lubrication system differs slightly from the test engine. A separate lubrication rig supply system was modeled to account for these differences. The rig supply model is used to model failures, allowing for temperature, pressure and flow affects to be observed. A failed O-ring was modeled in the bearing nozzles in the C-sump. The supply system was selected because of the high-pressure differential and the C-sump was selected because of the high soak back temperatures and ease of access in the rig.

**3.5.1.1 Assumptions.**—The assumptions made for engine, rig engine, and O-ring failure modeling purposes include:

- A single effective orifice can represent the equivalent line losses of multiple individual orifices.
- There is no entrance or exit losses were flows are mixed or split. Line losses occur only in pipe sections, orifices and coolers.
- Pressure drop across the engine oil cooler is modeled from the inlet to the A and B sump supply outlet. No pressure drop data is available for the additional cooler pressure drop in the between the A and B sump outlet and the C-sump outlet. Pressure drop across this section is assumed negligible.
- Effects of temperature and pressure are modeled separately in the engine oil cooler only. Effects of the temperature change on the pressure, and vice versa, are considered negligible.

**3.5.1.1.1. Failed O-ring assumptions:**

- A failed O-ring can be represented by an effective non-circular orifice.
- O-ring orifice exits into C-sump (internal to the sump, minimized detection).
- An O-ring failure will not affect the temperature or pressure of the sump pressurization air.

**3.5.1.2. Results.**—Supply temperatures in the model match engine data within 1°F. Pump discharge pressure, POE, and sump pressures correspond to engine data within <2 psi. The sum of all the pressure errors in the model converges to within 2 psi total (i.e., the sum of difference between the individual orifice outlet pressures feeding the sumps minus the corresponding sump calculated pressure are <<2 psi total).

**3.5.1.3. Conclusions.**—The lubrication supply model accurately represents a characteristic engine. This model can be used to accurately represent a lubrication system vehicle used for testing with minor alterations. The lubrication supply model can be modified to include failures that have been commonly seen on in the above paretos and the effect of the failure can be predicted in the lubrication system model.

**3.5.1.4. Rig model results.**—Oil supply temperatures in the rig model match engine simulated rig test data well. There is a discrepancy between the pump discharge pressure returned by the analytical model vs. the simulated rig test data of +7 psi. However, the pressure drop across the main supply pipes and the fuel/oil cooler correspond to the rig engine data. Therefore, the discrepancy is attributed to additional line losses in the rig test setup downstream of the fuel/oil cooler for which there was no rig test data available.

The oil supply rig model pressures matched rig test data well.

A non-production water/oil cooler was substituted on the rig for the production fuel/oil cooler used on the engine based on the test cell capability. The pressure and temperature drop across the rig cooler was less than that seen on the engine. A value based on the average value from rig engine data is read into the rig engine model for IRP and Idle conditions for the oil pressure at the main cooler exit and temperature at the main cooler exit and C-sump exit as there was not adequate rig test data to extrapolate a curve.

**3.5.1.5. Rig model conclusions.**—The lubrication system oil rig model accurately represents the rig test setup except for the noted 7 psi oil pressure discrepancy. This model can be modified to include failures that have been commonly seen from the above paretos. The 7 psid can be treated as an offset condition and us not expected to affect the results of the failure detection.

**3.5.1.6. Failed O-ring model.**—A failed O-ring model was modeled in the supply model of the C-sump. The O-ring is represented with an effective orifice of the O-ring gland. This would be a worse case scenario, where the O-ring in question is absent.

**3.5.1.7. Failed O-ring results.**—The analysis predicts the failure of an O-ring result in temperature, pressure and flow affects mainly in the C-sump, as shown in table 3.5.1.7–1.

TABLE 3.5.1.7-1.—FAILED O-RING RESULTS SUMMARY

	Flow [pph]	Supply Pressure [psia]		C-sump Temperature [°F]	
	Into C-sump	Master	C-sump	Supply	Scavenge
Predicted Delta	+315.3 pph	-9.2 psia	-9.21 psia	+7.7 °F	+0.4 °F
% Change	+22.6%	-7.8%	-12.3%	+3.7%	+0.2 %

### 3.5.2. Scavenge model

Due to the size of the lube system model, three sub-system models were created (the oil supply as mentioned previously, vented sump scavenge, and un-vented A-sump scavenge models). The models interact in an iterative process. The scavenge models' inlet oil temperature and pressure are defined from the supply model while the supply model's sump pressures are defined by the scavenge models. For these models, temperatures, pressures, and oil flows were taken from various sources (such as engine test data, the lube system schematic, drawings and drawing specifications) to accurately model the scavenge system of a characteristic engine.

A similar modeling approach was taken for the scavenge models in that an accurate engine scavenge model was developed and validated, the engine model was modified based on the differences in the lubrication system test rig, then common failures were modeled.

For the vented sump model, failures were initiated in the Aft C-sump which included a broken scavenge tube and a failed aft carbon seal. The aft carbon seal was chosen because of ease of accessibility in the test rig.

The C-Sump scavenge tube was chosen, again for ease of accessibility in the test rig and for the fact that this component is in the hot section where the majority of relative motion and thermal gradients exist, increasing the risk of failure.

**3.5.2.1. Assumptions.**—The assumptions made for all scavenge models for calculation purposes include:

- All air and oil exit the scavenge system through the vent and scavenge lines. Seal drains are not modeled. Seal drain effects on lube system pressures and temperatures are negligible
- The pressure drop seen across the A/O Separator in the AGB is a function of core speed and airflow through the separator.
- There is no non-circular compressible flow pipe section.
- Heat load to the sump is a function of windage, bearing heat generation, churning, sump wall conduction and can be modeled as a single heat load that varies with core speed.
- The flows through the carbon seals are modeled from the new seal leakage flow requirements listed in the seal specification (given temperature, pressure and flow limits). Effective circular areas were then back calculated to size an equivalent orifice and adjusted to take into consideration an internally calculated coefficient of discharge.
- There is no entrance or exit losses were flows are mixed or split. Line losses are modeled only in pipe sections and orifices.
- There is no heat addition in any of the pipe lengths (i.e., heat pickup through a strut).
- Oil is not being removed from the vent air exiting the A/O Separator in the AGB, so the model's oil consumption may appear high.

#### 3.5.2.1.1. Broken Scavenge Tube Assumptions:

- The inputs for air temperature and pressure surrounding the broken tube are the same air used for carbon seal pressurization.
- The air pressure surrounding the selected broken tube is greater than the pressure in the scavenge tube. For this reason, air flows into the tube and no air or oil leaks out.
- A broken scavenge tube causes reverse flow (flow into the sump and out the vent line). The effects of a broken scavenge tube are assumed to be equivalent to air being added to the sump. The line loss between the sump and the broken tube is neglected.

- The forward A-sump is un-vented and scavenged directly to a scavenge pump, it does not interact with the other sumps. Effects on secondary flow are neglected.

*3.5.2.1.2. Failed Carbon Seal Assumptions:*

- The A-sump is un-vented and scavenged directly to a scavenge pump, it does not interact with the other sumps. Effects on secondary flow are neglected.
- A carbon seal failure will not affect the temperature or pressure of the upstream supply air.

*3.5.2.1.3. Component Failure Assumptions:*

- The A-sump is un-vented and scavenged directly to a scavenge pump, it does not interact with the other sumps. Effects on secondary flow are neglected.
- A characteristic component failure is leaky a failed AGB carbon seal. These were modeled as an equivalent orifice defining a leakage rate from the AGB to ambient.

**3.5.2.2. Master engine scavenge model results.**—The Engine Lubrication Scavenge System consists of:

- A-sump – an un-vented sump, scavenged directly to the scavenge pump.
- B-sump – a vented sump with a direct scavenge.
- C-sump – a vented sump scavenged with a direct pump.
- AGB – a vented sump scavenged by a forward and an aft scavenge pump. The vent air passes through a dynamic air oil separator before being dumped overboard.

Each sump consists of: (1) the seal pressurization air, (2) the bulk supply oil, (3) the vent system, (4) the scavenge system, and (5) the sump.

Because the A-sump is un-vented and scavenged directly to the lube pump, it does not interact with the other sumps and is a separate scavenge model.

**3.5.2.3. Master engine scavenge model conclusions.**—The engine models were created because of the abundance of test data to validate the models. The above scavenge models accurately represent a characteristic military engine. With minor alterations, rig models have been created to simulate each of the above models.

**3.5.2.4. Lube test vehicle scavenge model results.**—A vented sump rig model was created based on the geometries represented in the engine model. However, the air and oil scavenge temperatures differ significantly from an engine on-wing. This is mainly due to the fact that there is no combustion occurring in the Lube Test Vehicle. Temperatures and pressures that were previously validated from engine test data are replaced and validated with Lube Test Vehicle data. The engine vented sump model ran at all speeds, however, the vented sump rig model was very sensitive to gain adjustments and would not converge at low core speeds, so due to time constraints the engine model was used to model failures. The vented sump rig model will run at high core speed scenarios (i.e., IRP conditions).

**3.5.2.5. Lube test vehicle model conclusions.**—More work is needed to adjust the gains in the vented sump scavenge model so it will run at low core speeds (idle). However once these gains are adjusted, it is expected that the model will match rig test data. The lube test vehicle inputs into the scavenge model accurately calculate temperatures, pressures and flows expected in the Lube Test Vehicle at IRP conditions. As done with the engine models, this analytical model of the test rig can be altered to model failures that have historically been encountered.

**3.5.2.6. Increased airflow failure vented sump model results.**—The plan was to create rig models which would change known items that are different from the engine, mostly temperatures and pressures of the sump buffer seal air and heat loads across the sump due to lack of combustion. The rig models were then be modified to include failures that have historically been identified by the oil system fault paretos described in section 3.3. However, due to time constraints, the rig models were concurrently developed while figuring out how to model failures on the engine models. As a result, the failed o-ring was modeled on the lube system rig model while the carbon seal failures and broken tube failure were modeled on the

engine model and not the rig model. With minimal time and effort, these failures can be incorporated into the rig model prior to testing and are not expected to have a large impact.

A carbon seal failure or a broken scavenge tube in the C-sump, each result in increase airflow into the sump.

- The broken scavenge tube is modeled as an unlimited air supply defined by temperature and pressure from pressure maps and the lubrication system schematic. The cracked tube is defined by an effective diameter and is assumed to act as an orifice.
- The failed carbon seal is modeled by increasing the effective diameter of the carbon seal (located in the C-sump).

An iterative process is used to accurately model pressure, temperature and flow responses to a failure. The oil temperature and flow data from the master supply model was input into the failure scavenge model. The scavenge model then performed its calculations and the sump pressures were used to run the supply model again. These supply temperatures and pressure were utilized in the scavenge model to predict the final temperatures within 0.2 percent and pressures within 1.5 percent.

The increased airflow failures show little change in temperature due to the additional air input. Realistic changes in temperature seen in the C-Sump and AGB vary by only several degrees because the specific heat and change in mass flow rate of air are much less than the specific heat and mass flow rate of oil.

Both failed models show large increases in pressure due to the additional air input

The increased airflow into the C-sump due to either failure results in large changes in pressure in any scavenge line or within any sump. These large changes in pressure can be measured in the B-sump, C-sump or AGB.

**3.5.2.3. Increased airflow failure model conclusions.**—Failure models of a carbon seal and a broken C-sump scavenge line showed large changes in pressure from characteristic engine data. The large changes in pressure show measurement of any of the vented sump scavenge pressures would indicate a failure of a main shaft carbon seal or broken sump tube.

Vent flow also showed a significant increase at IRP power with a large increase in equivalent carbon seal diameter. A flow measurement in the C-sump vent line may further identify the source of the problem based on the direction of flow.

### **3.6. Conclusion: Oil Systems**

Major faults of jet engine oil systems were characterized from historical fault databases. Physics based models were developed which adequately represented actual engine and rig test data. Physics based models were modified to detect major fault items. Sensors were selected to monitor major faults.

## **4. Subtask: Bearing System**

### **4.1. Background**

Main line engine bearings are inherently reliable; however the consequences of failure can be extremely high. Traditional bearing health monitoring has utilized magnetic chip detectors for decades. More recently (last 10 years or so) quantitative debris monitors have been introduced which provide an on-line indication of debris size and rate of production. These devices have proven very effective in detecting bearing spalling at a stage early enough to allow engine removal prior to significant secondary damage. One area where these devices have showed limitations however has been during failures of inter-shaft roller bearings. The configuration of these types of bearings, where both inner and outer races are rotating, can provide a tortuous path for failure debris to be transported. So, although the debris monitor is normally quite accurate, if there is no debris to detect, or the debris is flushed out when the debris monitor is inactive, it is rendered ineffective.

The main objective of this program was therefore to identify available sensors to develop a reliable bearing failure detection system, targeted at inter-shaft roller bearings. Additionally a demonstration of a conceptual design was also required.

## **4.2. Approach**

The overall requirements necessary for sensing bearing distress was defined. Criteria for selected sensors included the following:

- Measurements must provide advance warning of failure initiation.
- State-awareness sensors that are developed need to robustly survive the sump environment of future engines and
- Can be manufactured for reasonable costs.

An industry literature search related to main shaft bearing sensing/failures was conducted to identify the state of the art with respect to sensing technologies in this area. The most common failure mode considered for detection was surface or sub-surface initiated fatigue spalling, and the selected target application was an inter-shaft bearing. The inter-shaft differential bearing that is commonly used to support the HP rotor of any military engine provides significant challenge regarding sensor mounting and signal transmission.

A Sub-Contractor (The Timken Company) was added to the Team to assist GE with the design and testing aspects of the program. Timken is a bearing manufacturer and had a suitable rig test facility that was further modified to test the selected bearing. The Team completed a conceptual sensing design for this program. Hardware and instrumentation appropriate for a laboratory-grade test rig were procured. Testing of this conceptual design was then performed at Timken and the results analyzed.

## **4.3. Define Sensing Requirements**

Several different differential roller bearing configurations were reviewed. A literature search of different bearing failure modes and the failure detection approaches for the standard and differential roller bearings was conducted. Bearing failures remain one of the leading causes of In Flight Shut Downs (IFSD), and Unscheduled Engine Removals (UER). High-speed (ball and roller) bearings represent ~90 percent of failures. From a GE experience perspective, the vast majority of differential bearing failures result from outer race spallation. The leading failure cause being the bearing loads driving spall propagation from surface initiated damage. The inter-shaft bearing failures are the most difficult to detect with the conventional chip detection system because of a complex chip mobility within the rotating differential sump.

A variety of bearing fault detection techniques referred to in the literature, and sometimes successfully used in industrial bearing applications have not found much utilization with aircraft engine bearings.

The vibration diagnostics to identify a bearing fault becomes increasingly difficult under the aircraft engine core sump environment due to high speeds, presence of several frequencies (both synchronous, and non-synchronous), circuit path/lead-out complexities, and harsh thermal surroundings. The challenge to measure direct vibration signals from the distressed bearing becomes overwhelming when the bearing happens to be a differential with both the races rotating co- or counter-clockwise, and the sump configuration does not allow the mounting of any non-contacting probe. The targeted engine sump represents all these challenges. It is considered vital to develop and acquire as much bearing fault diagnostic data and experience for the complex configurations, if reliable prognostic approaches are to be viable. The team therefore identified the need to explore and evaluate other innovative means to monitor bearing health. These items included the measurement of lube supply and scavenge temperatures for a

particular sump, bearing outer race temperature data, the monitoring of strain gages, vibration signatures from accelerometers, and electrostatic debris monitoring.

#### **4.4. Identify Available Sensor Technologies**

The available sensor technologies to detect bearing spall initiation, progression, and overall damage accumulation was explored, however, the major emphasis was kept on the detection of initial spall or damage. As mentioned earlier, the bearing fault detection process for aircraft engine applications today do not utilize the available techniques widely used for the industrial applications. Given the complexities of any vibration based diagnostic scheme, and somewhat hostile sump operating environment, plus the fact that space is very limited and neither inner nor outer race is stationary, the existence of suitable sensors is also very limited. The need to develop some innovative differential bearing diagnostic system, and related sensors that can meet the challenges of an advanced engine sump design was realized. Several new concepts were explored and reviewed for its feasibility and merits. The GEAE engine development experience in terms of differential bearing instrumentation was utilized as guidance, and for a risk reduction approach.

Engine test instrumentation has been successfully applied to measure bearing performance under various engine operational conditions. Data from this instrumentation was transferred from the bearing to the data system via traditional slip ring technology. It is to be noted that for a long-term product application, neither the type/application of the sensors nor slip-ring technology is considered viable.

The finalized concept and the long-term design approach would be to use embedded sensors with internal telemetry to transfer information/power from the rotating domain to a static domain. This data would be finally transferred via a wired or wireless scheme to external processing resources.

Our current program work scope was inconsistent with the design of new sensors, and/or a related telemetry system. Therefore, the sub-contractor Timken was provided guidance to design a partial concept demonstration that could best meet the overall program objectives within the schedule and funding restraints.

Since the time-scale for Phase 1 of this program was very aggressive, and included a concept demonstration test, the team concluded that commercial of the shelf (COTS) slip ring technology would be used. The laboratory demonstration test did however incorporate sensors on the bearing outer race that rotated. The inner race for the demonstration was static (unlike a real differential bearing), in order to use existing (although modified) rig assets. The team down-selected the sensing needs to strain gages, thermocouples and accelerometers.

#### **4.5. Develop State-Awareness Sensors**

##### **4.5.1. Bearing outer race sensors**

The sensing design included the application of strain gages and thermocouples strategically located on the outside of the outer race of the test bearing. Additionally, accelerometers were also mounted on the outer race.

In order to obtain net effects due to a defect, testing was planned without and with a notched race. The Timken Co. therefore instrumented two bearing outer races; one of which had a single EDM slot machined axially across the raceway to simulate “damage.”

Each outer race was instrumented with 2 accelerometers, 2 thermocouples, and 7 strain gages. The placement of the strain gages was selected to provide responses at differing circumferential positions relative to the simulated damage site.

#### **4.5.2. Instrumentation system**

For the demonstration test a 14-channel COTS slip ring was procured. The sensing interconnection and data processing architecture for the demonstration test is illustrated in figure 4.5.2–1. Data collection capability to record all 11 sensors plus rig tachometer was provided by Timken.

#### **4.5.3. Test rig configuration**

An existing test rig at Timken was identified for use in this program. Traditional bearing test rigs drive the inner race of the bearing, while the outer race is stationary and is integrated into the rig structure. In order to test this sensing system in as realistic manner as practical, given the program timeframe, it was necessary to modify this Timken rig to drive the outer race of the test bearing and leave the inner race stationary. The rotation of the outer race provided the necessary speed and radial loading to stimulate the sensors. A view of the slip ring bearing assembly, mounted to the test rig arbor is shown in figure 4.5.3–1.

The fully assembled bearing test rig is shown in 4.5.3–2.

### **4.6. Demonstrate Sensing Concept in Laboratory Environment**

All testing was accomplished at Timken during the period April 2nd to April 30th, 2004.

#### **4.6.1. Test plan**

The demonstration testing was divided into 4 parts. Initial test runs served as a rig and instrumentation shakedown exercise. These tests explored the ranges of speed, load and lubrication of the planned tests. Part 2 of testing was with the undamaged bearing to obtain a set of baseline data. Part 3 of testing was a flatted roller installed in the undamaged bearing. The final part of the testing was a repeat of the test sequence performed for the undamaged bearing, but with the induced defect (notched) bearing.

#### **4.6.2. Test results and discussion**

All planned testing was successfully completed. No strain gages or thermocouples were lost during the testing. Both the undamaged and the EDM notch bearings showed no skidding damage on the raceways after the planned testing.

The following paragraphs discuss key observations from the acquired data for the different parts of the testing.

All strain gages showed 1/rev pulses as they passed through the radial load zone. Additionally most of the strain gages indicated secondary pulses indicative of number of rollers supporting the load.

The results were good for the evaluation of roller passing frequencies, and therefore determining the bearing slip rates at different conditions.

Figure 4.6.2–1 shows the measured roller passing frequency, compared with the zero slip theoretical value, and its variation as a function of different applied loads. Although not shown, these frequencies did not show any noticeable change as a result of the damage via flat roller or an EDM notch.

All strain gages showed good sensitivity with respect to increasing load and increased magnitude for the damaged race. The accelerometers showed a response separation between the two sensors for both the damaged configurations covering the flat roller as well as the EDM notch. The outer race temperature increase as a function of changing applied loads was observed for all cases.

The changes in average RMS strain values for the good and damaged bearings were distinguishable through out the range. The trend as well as the magnitudes of measured strains toward the max operating speed showed good sensitivity. The accelerometer response from both sensors was clearly distinct for the undamaged and damaged bearing.

Little sensitivity was observed for the strain gages or accelerometers toward the changing oil flows. A significant drop in the outer race temperatures as a function of increasing flow rate illustrated the improved cooling effect of the oil.

The survival of all the sensors and related instrumentation throughout the planned testing was indicative of a feasible robust sensing system package that could be developed for the future.

Comparison between the overall strain gage RMS amplitudes demonstrated a clear-cut distinction between the undamaged and damaged races.

The rotating strain gages performed well in assessing the roller passing frequencies, and the changes caused by the varying static, and dynamic loading and/or operating clearances.

The RMS values of micro strain of different strain gages at roller passing frequency were good indicators of the changing resultant loads. The wave pattern of the strain gage signal had useful information for diagnostics as well the prognostics aspects of a failing bearing.

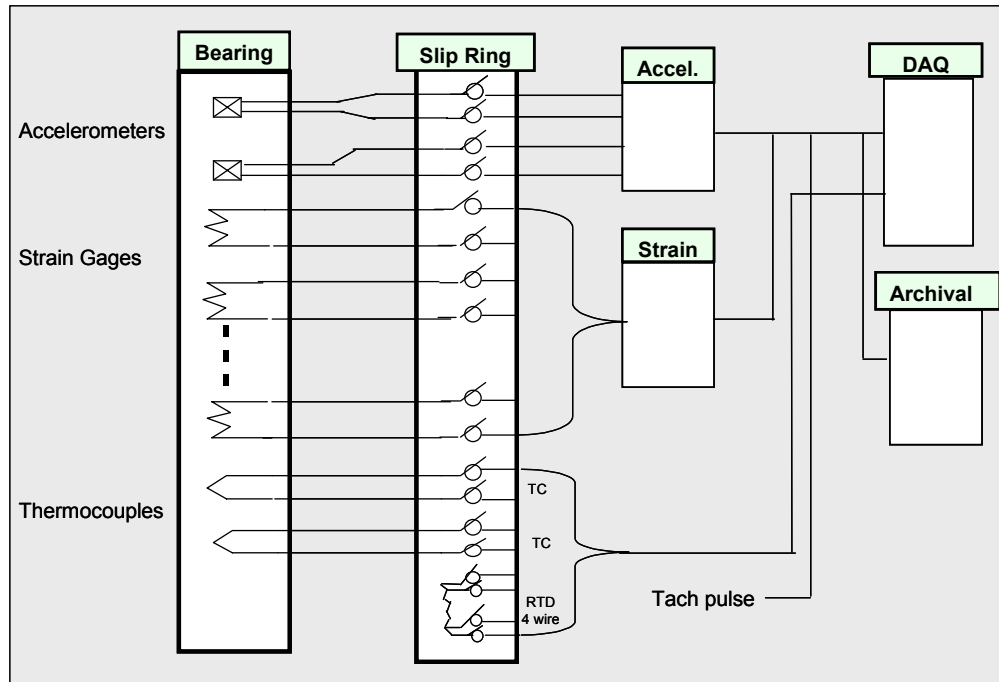


Figure 4.5.2-1.—Sensor interconnection and data processing.



Figure 4.5.3-1.—Test rig arbor and slip ring bearing sub-assembly.

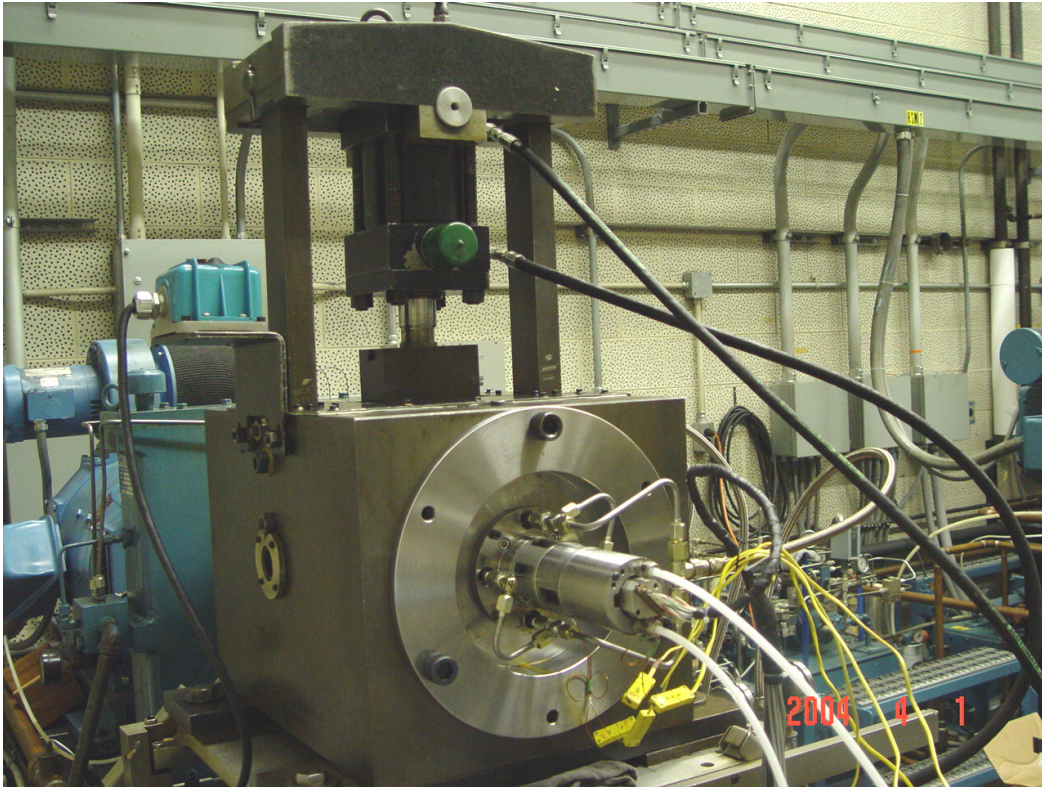


Figure 4.5.3-2.—Assembled bearing test rig.

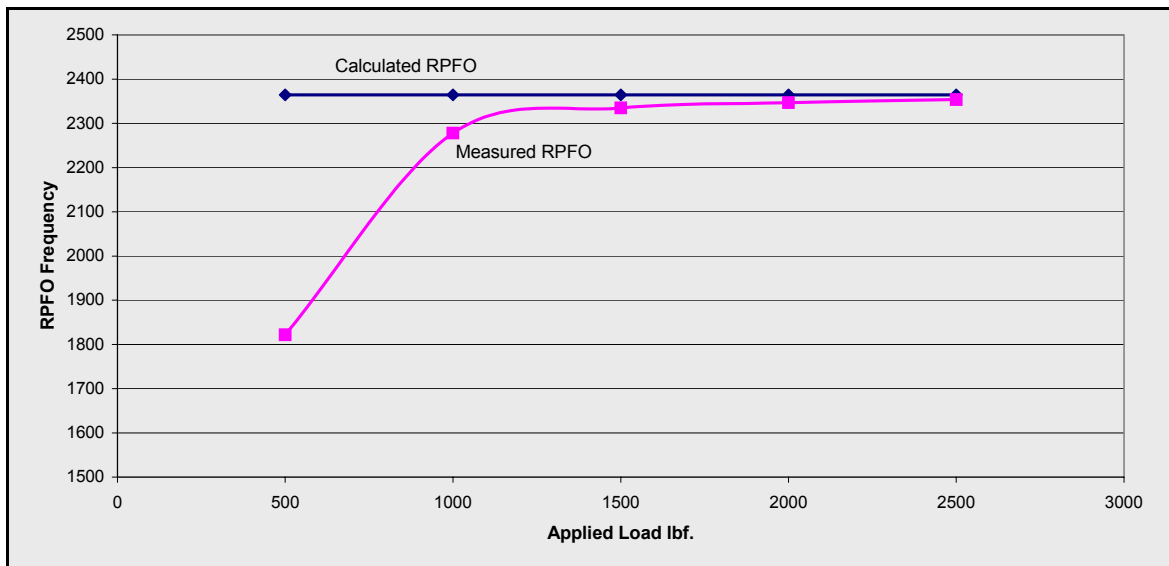


Figure 4.6.2-1.—Measured versus calculated RPFO (Undamaged Brg – constant speed).

## **5. Subtask: Fuel System**

### **5.1. Background**

Aircraft engine fuel system failures and subsequent troubleshooting cause a significant portion of the propulsion related airline delays and cancellations. The objective of this task was to develop a physics-based model of a commercial engine fuel system for the purpose of fault detection and isolation. The eventual goal is to reduce the maintenance and delays and cancellation.

### **5.2. Approach**

Key fuel system faults were identified via historical fault databases. These faults were reviewed for modeling suitability and a summary list down-selected. The GE commercial high bypass turbofan engine fuel system was selected for this program. The supplier chosen to support this effort (Argo-Tech) is a provider of some components for the chosen engine. The modeling effort was completed using GE's FuelSim modeling development environment. The scope of the modeling effort included all fuel system related components including actuators and heat exchangers.

### **5.3. Characterization of Major Faults of Jet Engine Starter and Ignition Systems**

The GE commercial engine database was utilized to identify engine fuel system repairs and maintenance on various fleets, covering the period 1997 to 2003.

The four most common fuel system components to experience maintenance action are the Hydro-mechanical Unit (HMU), fuel nozzles, fuel filter and Main Fuel Pump (MFP). The most common reason for maintenance action on the fuel filter is replacement due to clogging. This can easily be modeled. The reasons for maintenance on the remaining three components were further examined.

Most of the fuel nozzle problems were confined to a single engine type. A premature nozzle failure was prevalent throughout the fleet during initial operation. This unique problem was not selected for modeling.

The vast majority of the HMU removals occurred on specific engine type, however several root causes were identified and were considered general enough that they could be experienced on other applications. Problems with the various valves associated with the HMU were therefore selected for modeling.

With respect to Main Fuel Pump problems, the dominant fuel pump removal cause was for a fuel leak; a common problem across engine fleets. This failure mode was selected for modeling.

### **5.4. Develop Physics-Based Fault-Detection Model Requirements**

#### **5.4.1. Model Selection**

A high bypass turbofan engine fuel system was selected for this program. The supplier chosen to support this effort (Argo-Tech) is a provider of some components for the selected engine.

The selected fuel system comprises the following major components; Main Fuel Pump, Fuel Filter, Hydro-Mechanical Unit (includes bypass valve, fuel metering valve, etc.), Fuel Nozzles, Heat Exchangers, and various actuators for variable stator vanes, clearance control, etc.). A schematic of this system is illustrated in figure 5.4.1-1.

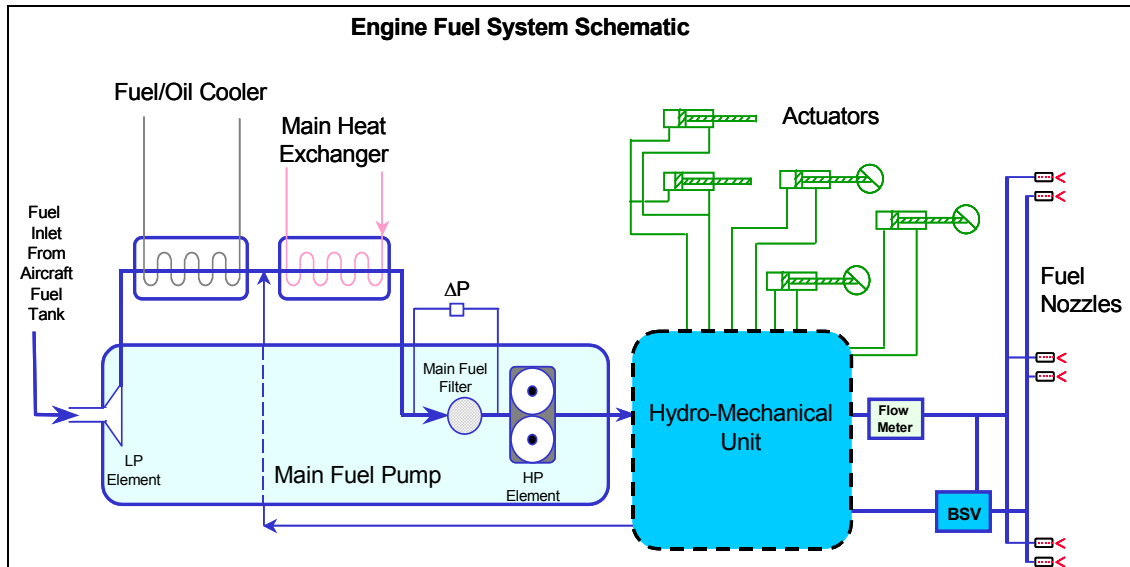


Figure 5.4.1-1.—Fuel system schematic.

### 5.4.2. General requirements

The model was implemented using GE's FuelSim simulation environment. The Argo-Tech Corporation supplied some of the model components, as follows:

- Main Fuel Pump
- Fuel Metering Valve
- Actuators (generic model)
- Heat Exchangers

The only component in the system that is prone to deterioration is the Main Fuel Pump. This was incorporated in the model as an efficiency loss, based upon historical data from Argo-Tech. The heat exchanger models were developed based upon the results of rig testing actual components.

In conjunction with the requirements for the general system model, several additional architectural requirements were placed on the Simulink models developed by ArgoTech. The ArgoTech models needed to comply with the formatting (inputs, outputs, ordering, etc.) currently in place in GE's FuelSim environment. Also, model inputs needed to be consistent with those already in the system.

The remainder of the system components was generated by GEAE, utilizing base components from the FuelSim library as well as developing new models for a pressurizing valve, a fuel flow transmitter and HMU leakage. GEAE also provided system level modeling and integration.

### 5.4.3. Model operating requirements

The model was designed to run at steady state conditions only, and over the complete engine flight envelope. The model represents the system as accurately as possible and was validated against engine test data.

The model has the capability to simulate the faults for MFP leakage, filter clogging and HMU leakage and valves; specifically Fuel Metering Valve, Bypass Valve, Burner Staging Valve. In addition, temperatures, pressures and flows are calculated at significant points in the system.

The boundary conditions (inputs) into this system are: inlet pressure and temperature, core speed, combustor pressure and nozzle fuel flow. These inputs must be input as time-snapshot data points. The system has the capability to process multipoint input (batch) data.

## 5.5. Modeling of The Fuel System For Real-Time Detection of Selected Faults

As indicated previously the modeling effort was divided between GEAE and Argo-Tech. Table 5.5–1 summarizes the tasks completed by each contributor.

TABLE 5.5–1.—FUEL SYSTEM MODELING TASKS

GE Aircraft Engines	The Argo-Tech Corporation
Model Development: <ul style="list-style-type: none"> <li>○ HMU leakage</li> <li>○ Fuel flow transmitter</li> <li>○ Downstream subsystem, including fuel nozzles</li> </ul>	Model Development: <ul style="list-style-type: none"> <li>○ Main fuel pump</li> <li>○ Fuel metering valve</li> <li>○ Heat exchangers</li> <li>○ Generic actuator</li> </ul>
Modified models for the FUELSIM environment: <ul style="list-style-type: none"> <li>○ Main fuel pump</li> <li>○ Fuel metering valve</li> <li>○ Heat exchangers</li> <li>○ Generic actuators</li> </ul>	Performed: <ul style="list-style-type: none"> <li>○ Rig testing to determine heat exchanger performance</li> <li>○ Derivations for equations for effectiveness and pressure drops</li> </ul>
Upgraded FUELSIM models: <ul style="list-style-type: none"> <li>○ Pressurizing valve</li> <li>○ Bypass valve</li> </ul>	Provided: <ul style="list-style-type: none"> <li>○ Main fuel filter and wash screen pressure drops</li> <li>○ Other engine fuel pump model for comparison efforts.</li> </ul>
System Level Tasks: <ul style="list-style-type: none"> <li>○ Integrated all component models</li> <li>○ Added fault injection capability</li> <li>○ Matched system pressures to engine test data</li> </ul>	

### 5.5.1. Argo-tech models

All of Argo-Tech models were developed using Matlab version 6.5.1 and Simulink version 5.1.

1. The main fuel pump is actually a composite component that includes a boost pump, gear pump, relief valve, wash flow filter and main fuel filter.
2. The Fuel Metering Valve is not manufactured by Argo-Tech, however they had interest in generating a model for this component. GEAE therefore provided high-level specification information relative to this valve.
3. There are several actuators in the selected engine fuel system. Argo-Tech was tasked with generating a generic actuator model that could then be utilized for multiple instances in the overall system model at GEAE. Figure 5.5.1–1 illustrates the top level Simulink model for the generic actuator.

- The team did not have thermal performance data readily available for the heat exchangers in the selected fuel system. Argo-Tech did have examples of these components in their fuel system rig. It was decided that Argo-Tech should run a series of rig tests to generate basic thermal data for these heat exchangers. The test setup is shown in figure 5.5.1-2.

An example of typical data collected for the heat exchangers is included as figure 5.5.1-3 and figure 5.5.1-4. The resulting Simulink top-level model for this component then included as figure 5.5.1-5. Similar data and models were developed for the IDG and servo heat exchangers.

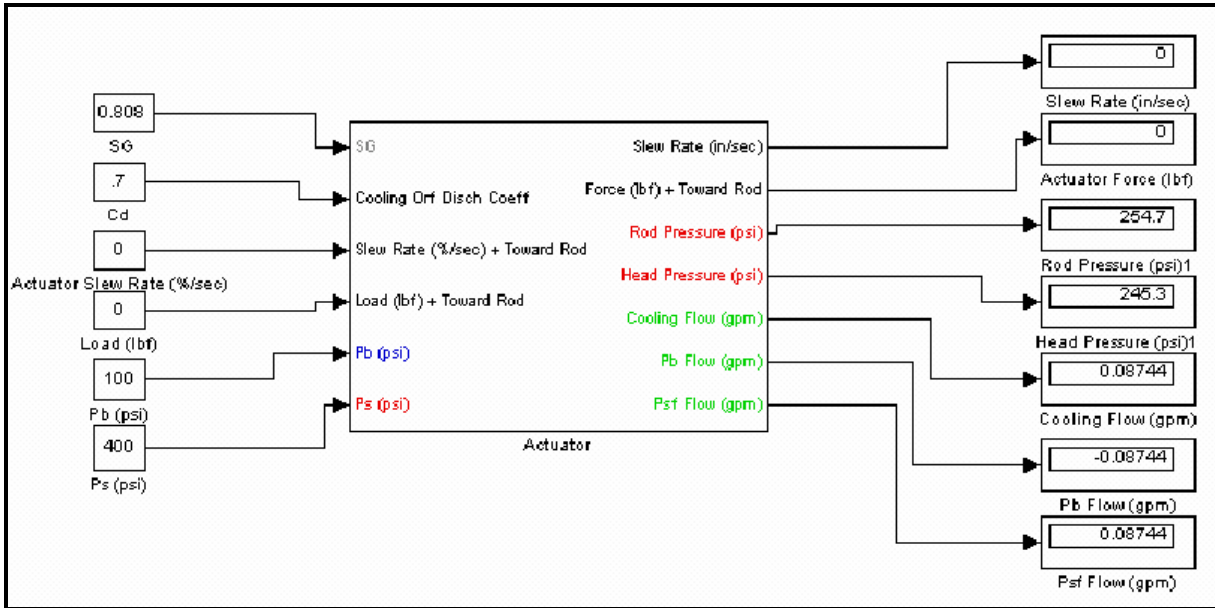


Figure 5.5.1-1.—Generic actuator top-level model representation.

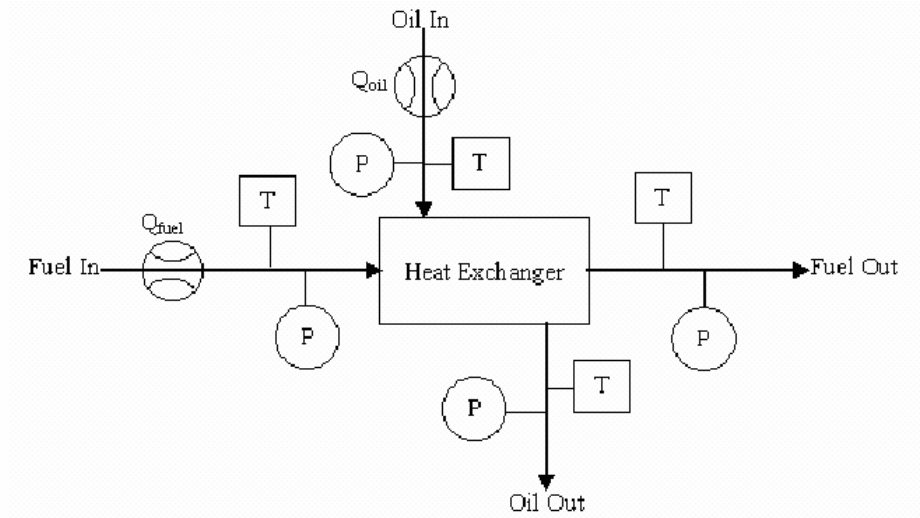


Figure 5.5.1-2.—Heat exchanger test circuit.

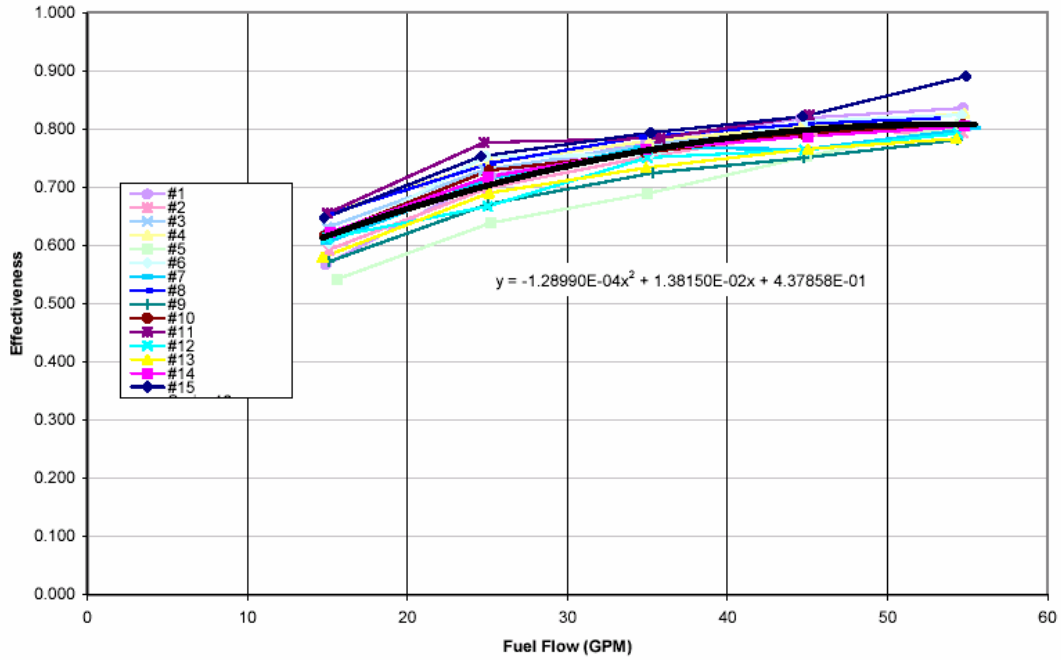


Figure 5.5.1-3.—Example heat exchanger effectiveness versus fuel flow.

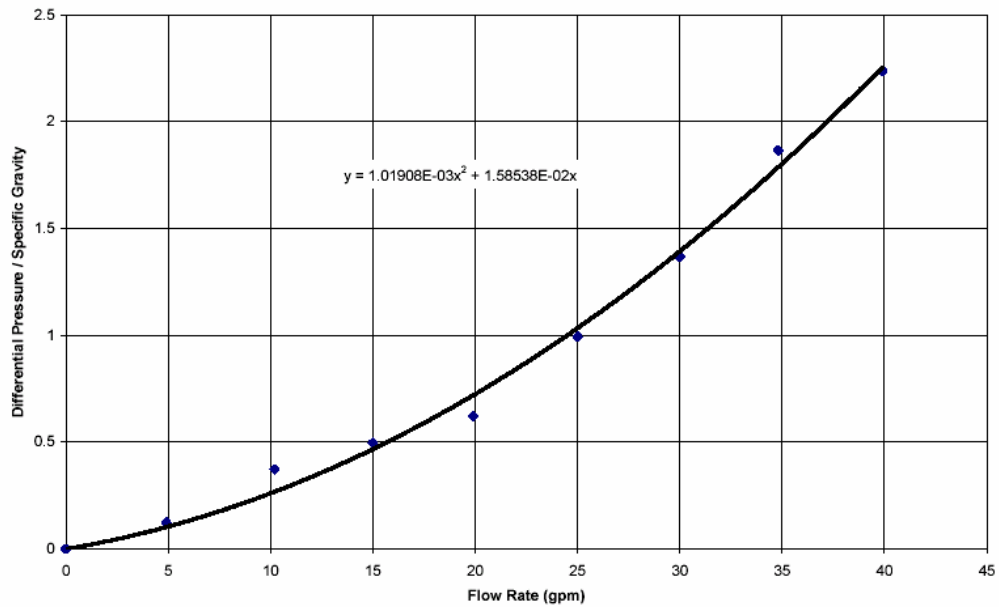


Figure 5.5.1-4.—Example heat exchanger pressure drop characteristic.

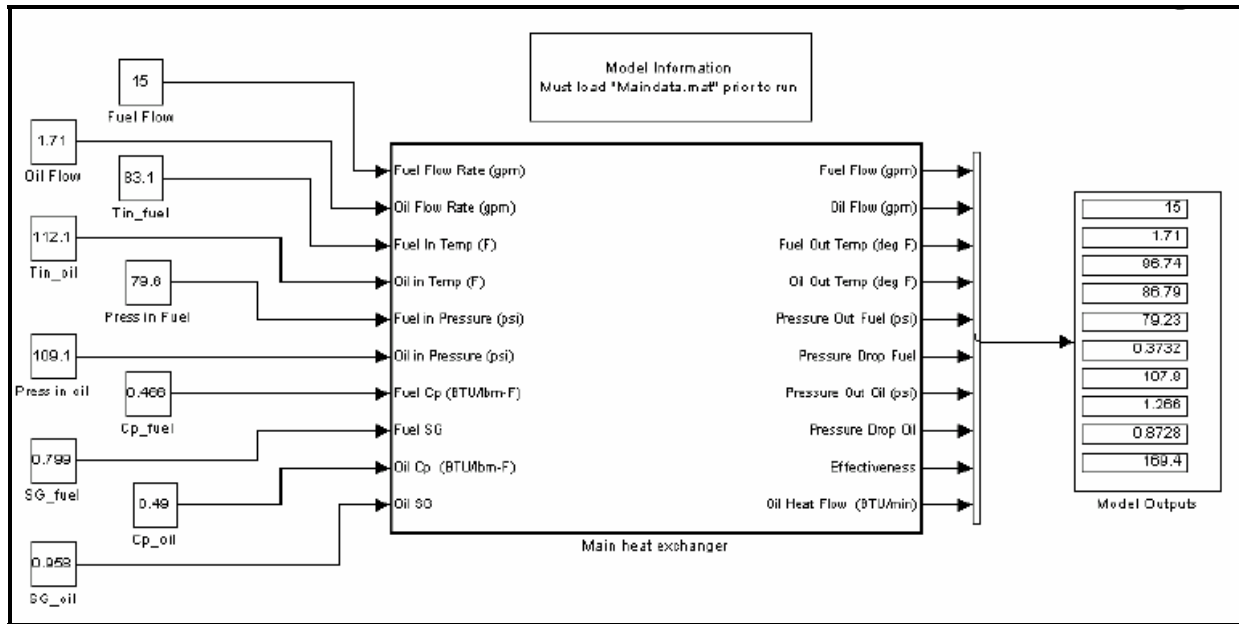


Figure 5.5.1-5.—Example heat exchanger top-level model representation.

### 5.5.2. GEAE models

GEAE generated a two new component models and made changes to others as follows:

1. The fuel flow transmitter is a component that was not available in the FuelSim library. Shown in figure 5.5.2-1 is the flow pressure relationship on which the component model was based.
2. A standard (empirically derived) pressurizing valve model had previously been developed for the FuelSim library. A new physics-based model was developed for this program. This new model uses pressure, flow, and spring parameters to balance the valve.
3. The portion of the system, downstream from the HMU utilized basic fuel nozzle manifold, nozzle filter and burner staging valve FUELSIM components, plus the new flow-meter model. The nozzle pressure drops were derived from measured data. A pressure adjustment to compensate for increased pressure drops at higher fuel flows associated with piping was also added. Finally, PS3 had to be corrected for the static pressure profile difference between the PS3 sensor and the fuel nozzle discharge. The final correlation between the measured values and the model is shown in figure 5.5.2-2.

### 5.5.3 Fault injection capability

The following fault injection capability was incorporated in to the system model, or components are necessary.

1. Main Fuel Pump Fuel Leak:  
Leakage is standard FuelSim component modeling feature. Inputs include leak diameter, shape and ambient pressure.
2. Fuel Metering Valve Fault:  
The FMV model designed by Argo-Tech has the capability for a position override which will set the FMV at a certain position, which can be used to model a stuck FMV.
3. Bypass Valve Faults:  
The bypass valve has an input to determine the amount of flow going to the fuel nozzles. This value is taken from the test data and is listed in the input file. This valve can be offset by adding a

set amount to all nozzle flows in the input file or can be modeled as stuck by entering one set value in the input file for nozzle flow.

4. Burner Staging Valve:

The BSV can be set as open, closed, or can be set so that it opens once a certain fuel flow is reached. Therefore to model faults we can model the valve stuck open, closed, or with automatic opening at some other point that what the valve should be set.

5. Clogged Fuel Filter:

A clogged filter can be modeled simply by changing the filter coefficients, which will change the pressure drop across the filter.

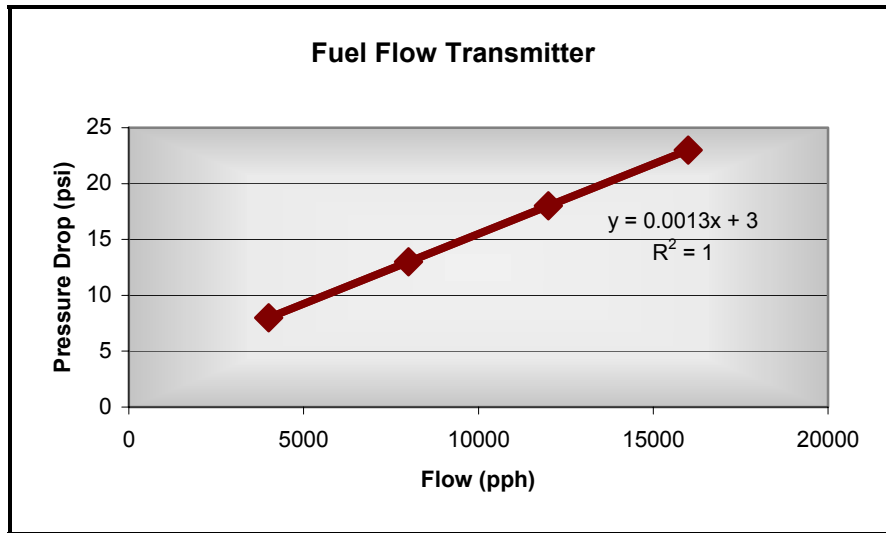


Figure 5.5.2-1.—Fuel flowmeter pressure drop characteristics.

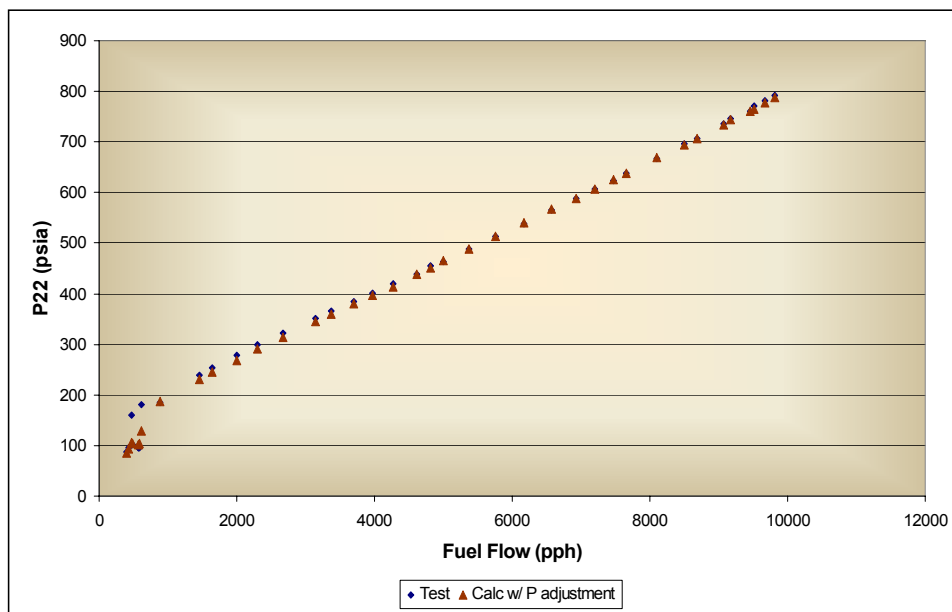


Figure 5.5.2-2.—Manifold pressure characteristic comparison.

**REPORT DOCUMENTATION PAGE***Form Approved*  
*OMB No. 0704-0188*

Public reporting burden for this collection of information is estimated to average 1 hour per response, including the time for reviewing instructions, searching existing data sources, gathering and maintaining the data needed, and completing and reviewing the collection of information. Send comments regarding this burden estimate or any other aspect of this collection of information, including suggestions for reducing this burden, to Washington Headquarters Services, Directorate for Information Operations and Reports, 1215 Jefferson Davis Highway, Suite 1204, Arlington, VA 22202-4302, and to the Office of Management and Budget, Paperwork Reduction Project (0704-0188), Washington, DC 20503.

<b>1. AGENCY USE ONLY (Leave blank)</b>		<b>2. REPORT DATE</b> October 2005	<b>3. REPORT TYPE AND DATES COVERED</b> Final Contractor Report	
<b>4. TITLE AND SUBTITLE</b>  Intelligent Engine Systems Work Element 1.3: Sub System Health Management			<b>5. FUNDING NUMBERS</b>  WBS-22-714-92-50 NAS3-01135	
<b>6. AUTHOR(S)</b>  Malcolm Ashby, Jeffrey Simpson, Anant Singh, Emily Ferguson, and Mark Frontera				
<b>7. PERFORMING ORGANIZATION NAME(S) AND ADDRESS(ES)</b>  General Electric Aircraft Engines One Neumann Way Cincinnati, Ohio 45215-1915			<b>8. PERFORMING ORGANIZATION REPORT NUMBER</b>  E-15281	
<b>9. SPONSORING/MONITORING AGENCY NAME(S) AND ADDRESS(ES)</b>  National Aeronautics and Space Administration Washington, DC 20546-0001			<b>10. SPONSORING/MONITORING AGENCY REPORT NUMBER</b>  NASA CR-2005-213965	
<b>11. SUPPLEMENTARY NOTES</b> Malcolm Ashby, Jeffrey Simpson, Anant Singh, and Emily Ferguson, General Electric Aircraft Engines, One Neumann Way, Cincinnati, Ohio 45215-1915; and Mark Frontera, General Electric Global Research Center, One Research Circle, Niskayuna, New York 12309. Project Manager, Clayton L. Meyers, Aeronautics Division, NASA Glenn Research Center, organization code PRV, 216-433-3882.				
<b>12a. DISTRIBUTION/AVAILABILITY STATEMENT</b>  Unclassified - Unlimited Subject Category: 07  Available electronically at <a href="http://gltrs.grc.nasa.gov">http://gltrs.grc.nasa.gov</a> This publication is available from the NASA Center for AeroSpace Information, 301-621-0390.			<b>12b. DISTRIBUTION CODE</b>	
<b>13. ABSTRACT (Maximum 200 words)</b>  The objectives of this program were to develop health monitoring systems and physics-based fault detection models for engine sub-systems including the start, lubrication, and fuel. These models will ultimately be used to provide more effective sub-system fault identification and isolation to reduce engine maintenance costs and engine down-time. Additionally, the bearing sub-system health is addressed in this program through identification of sensing requirements, a review of available technologies and a demonstration of a demonstration of a conceptual monitoring system for a differential roller bearing. This report is divided into four sections; one for each of the subtasks. The start system subtask is documented in section 2.0, the oil system is covered in section 3.0, bearing in section 4.0, and the fuel system is presented in section 5.0.				
<b>14. SUBJECT TERMS</b>  Propulsion systems (aircraft)			<b>15. NUMBER OF PAGES</b> 38	
			<b>16. PRICE CODE</b>	
<b>17. SECURITY CLASSIFICATION OF REPORT</b> Unclassified	<b>18. SECURITY CLASSIFICATION OF THIS PAGE</b> Unclassified	<b>19. SECURITY CLASSIFICATION OF ABSTRACT</b> Unclassified	<b>20. LIMITATION OF ABSTRACT</b>	



